THE JOURNAL OF BIOLOGICAL CHEMISTRY
Vol. 278, No. 50, Issue of December 12, pp. 50175–50181, 2003

Printed in U.S.A.

CD and NMR Studies of Prion Protein (PrP) Helix 1

NOVEL IMPLICATIONS FOR ITS ROLE IN THE $PrP^C \rightarrow PrP^{Sc}$ CONVERSION PROCESS*[S]

Received for publication, May 19, 2003, and in revised form, August 6, 2003
Published, JBC Papers in Press, September 2, 2003, DOI 10.1074/jbc.M305234200

Jan Ziegler, Heinrich Sticht‡, Ute C. Marx, Wolfgang Müller, Paul Rösch, and Stephan Schwarzinger§

From the Lehrstuhl für Biopolymere, Universität Bayreuth, 95447 Bayreuth, Germany and ‡Institut für Biochemie, Abteilung für Bioinformatik, Friedrich-Alexander-Universität, 91054 Erlangen, Germany

The conversion of prion helix 1 from an α-helical into an extended conformation is generally assumed to be an essential step in the conversion of the cellular isoform PrP^C of the prion protein to the pathogenic isoform PrP^{Sc}. Peptides encompassing helix 1 and flanking sequences were analyzed by nuclear magnetic resonance and circular dichroism. Our results indicate a remarkably high instrinsic helix propensity of the helix 1 region. In particular, these peptides retain significant helicity under a wide range of conditions, such as high salt, pH variation, and presence of organic co-solvents. As evidenced by a data base search, the pattern of charged residues present in helix 1 generally favors helical structures over alternative conformations. Because of its high stability against environmental changes, helix 1 is unlikely to be involved in the initial steps of the pathogenic conformational change. Our results implicate that interconversion of helix 1 is rather representing a barrier than a nucleus for the $PrP^C \rightarrow PrP^{Sc}$ conversion.

Prion protein, PrP,[1] is probably the disease-causing agent of transmissible spongiform encephalopathies such as bovine spongiform encephalopathy in cattle or Creutzfeldt-Jakob disease in man (1). Its cellular form, PrP^C, is a highly conserved cell surface glycoprotein of 230 amino acids expressed in all of the mammals studied so far as well as in several species of fish and birds (2, 3). The physiological function of PrP^C is not yet fully understood. PrP^C seems to be involved in the maintenance of proper presynaptic copper levels as well as in protecting neurons from oxidative stress (4, 5). In addition, the physiological function of PrP^C could be associated with higher neurological functions such as learning and memory (5). According to the protein-only hypothesis, disease is caused by accumulation of a misfolded pathogenic isoform, PrP^{Sc}, which is the result of an irreversible large scale conformational change of PrP^C. Although PrP^C is largely α-helical and soluble in polar solvents and sensitive to protease K digestion, PrP^{Sc} consists mostly of β-sheets, is soluble only in nonpolar, denaturing solvents, and is resistant to digestion with protease K (6). PrP^{Sc} forms fibrillar aggregates similar to other amyloid fibrils (7). Accumulation of PrP^{Sc} aggregates is accompanied by astrocytosis and gliosis in central nervous tissue, which in turn result in vacuoles in the brains of patients.

The solution structures of human PrP-(23–230), huPrP (8), mouse PrP-(121–231) (9), bovine PrP-(23–230) (10), and Syrian hamster PrP-(29–231) (11) have been determined by NMR spectroscopy. They possess a high degree of structural conservation consistent with the high sequence identity of these proteins. Prion proteins consist of a flexible NH_2-terminal domain spanning residues 23–124 ($huPrP^C$-numbering scheme), which is largely disordered. This region includes an octapeptide sequence that is repeated four times from residues 60 to 92 and that is likely to bind copper (4). This part also contains the palindromic sequence, AGAAAAGA, which may be involved in fibrillogenesis (12). The COOH-terminal domain (residues 125–231) adopts a well defined tertiary structure containing three α-helices and a short anti-parallel β-sheet. This globular domain can further be divided into two subdomains, one long hairpin subdomain (helix 1 and the β-sheet) and one purely α-helical subdomain (helices 2 and 3) (13). In contrast, little is known regarding the structural properties of PrP^{Sc}. Epitope mapping of the PrP^{Sc}-specific monoclonal antibody 15B3 suggests a structural rearrangement of the sequence of helix 1 during the conversion reaction (14). A recent low resolution model derived from electron-crystallographic data proposes incorporation of the unstructured domain and the long hairpin subdomain into a left-handed β-helix while the helical subdomain is supposed to retain its structure (15). These data suggest that helix 1 has to undergo a major structural rearrangement from an α-helix into a structure involving a significant amount of β-sheet (Scheme 1). In addition, helix 1 possesses several other unique features. Helix 1 extends from Asp-144 to Met-154 in the mean NMR structure of human prion protein (8). 6 of these 11 residues are charged at neutral pH making helix 1 the most hydrophilic helix in all of the known protein structures (16). Furthermore, helix 1 has very few long range interactions. Moreover, it has a significant number of solvent-accessible backbone hydrogen bonds (17). On the basis of computational studies, it has been hypothesized that helix stabilization occurs electrostatically via two intrahelical salt bridges and a charge distribution interacting favorably with the intrinsic dipole moment of the helix (16). To further investigate the intrinsic conformational propensity of the sequence of helix 1, we conducted NMR spectroscopic and computational studies of

* This work has been supported by Grant "Bay 2-1528000121" from the Bavarian Ministery for Science, Research, and Art. The costs of publication of this article were defrayed in part by the payment of page charges. This article must therefore be hereby marked "*advertisement*" in accordance with 18 U.S.C. Section 1734 solely to indicate this fact.

[S] The on-line version of this article (available at http://www.jbc.org) contains supplemental data.

§ To whom correspondence should be addressed: Lehrstuhl Biopolymere, Universität Bayreuth, D-95440 Bayreuth, Germany. Tel.: 49-0-921-55-2046; Fax: 49-0-921-55-3544; E-mail: stephan.schwarzinger@uni-bayreuth.de.

[1] The abbreviations used are: PrP, prion protein; PrP^C, cellular prion protein; PrP^{Sc}, scrapie-associated prion protein; NMR, nuclear magnetic resonance; TOCSY, total correlation spectroscopy; PDB, Protein Data Bank; NOESY, nuclear Overhauser effect spectroscopy; CSI, chemical shift index; CD, circular dichroism; huPrP, human prion protein; NOE, nuclear Overhauser effect; TFE, trifluoroethanol.

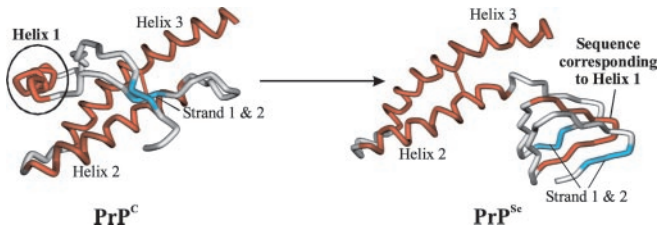

SCHEME 1. **Schematic view of the structural conversion of PrP^C into pathogenic PrP^{Sc}.** A main problem in prion diseases is to understand the conformational change from cellular PrP^C into the amyloid-forming infectious PrP^{Sc} conformation. Shown are the structure of the carboxyl-terminal domain of PrP^C (solution structure, PDB entry 1QLX (8)) and a structural model of PrP^{Sc} for the corresponding amino acid sequence. This schematic model of PrP^{Sc} is based on low resolution electron crystallography data and homology modeling as proposed by Wille *et al.* (15). Secondary structure elements are color-coded according to their occurrence in the solution structure of the cellular conformation (*red* = α-helix; *cyan* = β-sheet). Whereas helices 2 and 3 remain helical in PrP^{Sc}, helix 1, which is *encircled* in the structure of PrP^C, is incorporated into the left-handed β-helix that builds up the amino-terminal part of PrP^{Sc}. The images were created with WebViewer 5.0 lite (Accelrys, San Diego, CA).

several synthetic peptides encompassing helix 1 and flanking sequences.

EXPERIMENTAL PROCEDURES

Peptides—All of the peptides were purchased from Jerini AG (Berlin, Germany) as high pressure liquid chromatography-purified freeze-dried powder containing trifluoroacetate as counterions. Peptides were protected by an NH_2-terminal acetyl group and by amidation at the COOH terminus to exclude charge effects from free termini. The peptides under investigation were as follows: huPrP-(110–157) (Ac-KHMAGAAAAGAVVGGLGGYMLGSAMSRPIIHFGSDYEDRYYRENMHRY-NH_2); huPrP-(140–158) (Ac-HFGSDYEDRYYRENMHRYP-NH_2); and huPrP-(140–166) (Ac-HFGSDYEDRYYRENMHRYPNQVYYRPM-NH_2).

NMR-Spectroscopy—For the preparation of NMR samples, the freeze-dried peptides were dissolved in H_2O/D_2O (9:1) buffered by 25 mM sodium acetate for pH 4.5 samples or 10 mM potassium phosphate for pH 6.5 samples. 0.1% sodium azide was used to prevent bacterial growth in the sample. Undissolved material was removed by centrifugation, and the pH value of the solution was readjusted. Samples contained 2,2-dimethyl-2-silapentane-5-sulfonate as internal reference for proton chemical shifts. Peptide concentrations were determined photospectrometrically using a molar absorption coefficient ϵ_{280} of 1280 cm^{-1} per tyrosine residue (18). Spectra were recorded on Bruker Avance 400 and DRX600 spectrometers with proton frequencies of 400 and 600 MHz, respectively. Quadrature detection in f1 was achieved using States-time-proportional phase incrementation or the echo-anti-echo method. The solvent signal was suppressed by the WATERGATE W5 method (19, 20) or by excitation sculpting (21). Two-dimensional ^1H-^1H TOCSY (22) spectra with mixing times of 40 and 80 ms, respectively, and two-dimensional ^1H-^1H NOESY (23) spectra with mixing times of 150 and 300 ms, respectively, were recorded at 283 K. The temperature was calibrated with methanol (24). Data were processed with the software package NDEE (Spin Up Inc., Dortmund, Germany). Typically, a sine-squared window function shifted by $\pi/3$ was applied in both dimensions with zero-filling to 1024 data points in f1 and 4096 data points in f2. Base-line correction (25) was performed using home-written software. Sequential assignments were achieved using the main-chain-directed strategy devised by Wüthrich *et al.* (26). Assignment of secondary structure elements was achieved using the $^1H^\alpha$ chemical shift index (CSI) method described by Wishart *et al.* (27). Random coil chemical shifts derived from Ac-GGXGG-NH_2-type model peptides acquired under acidic conditions and their corresponding correction factors correcting for effects from the local amino acid sequence were employed (28, 29). For studies at higher pH values, random coil chemical shifts for Asp and Glu were taken from Ac-GG(D/E)AGG-NH_2 peptides measured at pH 5 (30).

CD Spectroscopy—CD spectra were recorded on a Jasco J810 instrument using quartz cells with path lengths of 0.1 and 1 mm, respectively. Samples were prepared from the NMR samples by dilution with appropriate buffers. Spectra were taken at 283 K. Typically, four scans over the wavelength range 200–260 nm were acquired with a stepwidth of 0.5 nm, an integration time of 4 s, and a bandwidth of 1 nm. Helix contents were estimated from the mean residual ellipticity at 222 nm (31).

Pattern Search—Proteins containing a pattern of charged residues similar to that of huPrP helix 1 were identified by a pattern search against the Protein Data Bank (PDB) filtered at 95% sequence identity (PDB95) using the program PATTINPROT (npsa-pbil.ibcp.fr/cgi-bin/npsa_automat.pl?page = /NPSA/npsa_pattinprot.html). In addition to the pattern [DE]-*X*-*X*-[DE]-[RK]-*X*-*X*-[RK] present in huPrP, three additional patterns generated by permutation of the charged residues ([DE]-*X*-*X*-[RK]-[RK]-*X*-*X*-[DE],[RK]-*X*-*X*-[DE]-[DE]-*X*-*X*-[RK],and[RK]-*X*-*X*-[RK]-[DE]-*X*-*X*-[DE]) were used as input. All four patterns are formed by two overlapping subpatterns, each containing a positively and a negatively charged residue four positions apart in sequence. In addition, the patterns [DE]-*X*-*X*-[DE]-[RK]-*X*-*X*-[RK]-[DE], [DE]-*X*-*X*-A-[RK]-*X*-*X*-[RK]-[DE], and [DE]-*X*-*X*-[DE]-[RK]-*X*-*X*-[RK]-A were used to assess the effect of point mutations on helix propensity. Secondary structure of the residues forming these patterns was analyzed using home-written software that correlates the PATTINPROT output (PDB code and sequence position of the pattern) with the secondary structure of the corresponding residues obtained from dictionary of secondary structure of proteins analysis (32). The type of secondary structure and the accessible surface area for each position of the pattern and the flanking residues were calculated.

RESULTS AND DISCUSSION

Stability of Helix 1 Is Independent of Neighboring Sequences—The effect of flanking sequences on the conformational properties of helix 1 in the three peptides, huPrP-(110–157), huPrP-(140–158), and huPrP-(140–166), was analyzed by means of CD and NMR spectroscopy. Because of the low solubility of huPrP-(110–157) and huPrP-(140–166) at near-neutral pH values, investigations had to be carried out at pH 4.5. Information on the preference for a particular secondary structure was determined using $^1H^\alpha$ chemical shifts (27, 28). In all of the three peptides, chemical shift analysis indicates the presence of helical conformation in the region 145–155, which is in good agreement with the position of helix 1 in the solution structure of huPrP-(90–231) (Table I). $^1H^\alpha$ chemical shifts for helix 1 in the three peptides show no significant differences, implying that the sequences flanking helix 1 neither contribute to its stability nor to its conformational preference. However, sequences adjacent to helix 1 behave as free flight random coils. In particular, the sequence 129–131, forming β-strand 1 in the native PrP^C structure, does not show any sign of populating an extended conformation (Fig. 1, *A* and *B*). Moreover, the NH_2-terminal alanine-rich region, which is thought to play a key role in fibril formation (33), does not populate extended conformations nor does it form helical conformations as might be expected from the high content of alanine residues. An exception from random coil behavior is found for the sequence prior to the NH_2 terminus of helix 1 in which a small population of extended conformation can be found. However, the absence of tertiary NOE-cross-peaks in the peptides suggests high conformational flexibility.

CD spectra of the peptides huPrP-(140–158) and huPrP-(140–166) show a broad negative band at 208 nm with a shoulder at 216 nm, indicating the presence of some regular secondary structure, whereas the spectrum of huPrP-(110–157) resembles more that of a random coil (Table I, full spectra are shown in supplemental information). The helix content of the peptides, as estimated from the residual ellipticity at 222 nm, amounts to 4% for huPrP-(110–157), 7% for huPrP-(140–158), and 6% for huPrP-(140–166) (Table I). CD spectroscopy shows consistently lower helix content than NMR spectroscopy because the CD signal represents an average over the entire peptide while NMR reports the helix content at a particular position. In addition, the high number of tyrosine residues in the peptides may lead to non-trivial CD spectra, thereby causing misestimation of secondary structure content (34).

To further explore the conformational properties as a func-

TABLE I
Average helix content of the investigated peptides

n/a, not available.

	CD[a]	NMR (total)[b]	NMR-(144–154)[c]	AGADIR[d]
huPrP-(110–157), pH 4.5	0.04	0.14	0.43	0.04
huPrP-(140–158), pH 4.5	0.07	0.27	0.46	0.1
huPrP-(140–166), pH 4.5	0.06	0.21	0.46	0.07
huPrP-(140–158), pH 2.0	0.08	0.17	0.27	0.03
huPrP-(140–158), pH 6.5	0.14	0.34	0.58	0.14
huPrP-(140–158), pH 4.5, 250 mM NaCl	n/a	0.24	0.41	0.1
huPrP-(140–158), pH 4.5, 500 mm NaCl	n/a	0.28	0.45	0.09
huPrP-(140–158)D147A, pH 4.5	0.13	0.34	0.52	0.11
huPrP-(140–158)E152A, pH 4.5	0.09	0.29	0.44	0.07
huPrP-(110–157), 40% acetonitrile	0.08	0.03	0.37	n/a
huPrP-(110–157), 40% TFE	0.11	n/a	n/a	n/a
huPrP-(140–158), 40% TFE	0.32	0.37	0.66	n/a

[a] Estimated from $[\theta]_{222\ nm}$ (31).
[b] Estimated from the average secondary structure shift for all of the residues.
[c] Estimated from the average secondary structure shift for residues 144–154.
[d] Calculated by AGADIR (40, 41, 42).

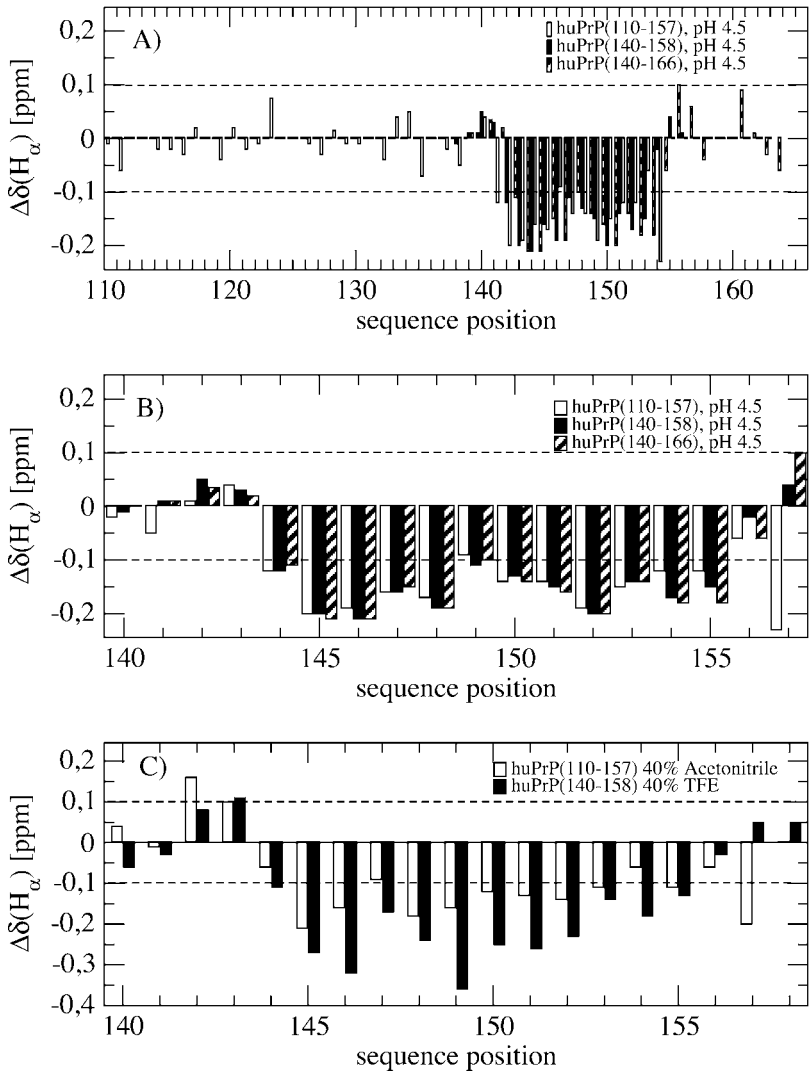

FIG. 1. **Context and solvents dependence of $^1H^\alpha$ secondary shifts.** *A*, comparison of the $^1H^\alpha$ shifts for the region 110–166. Difference of $^1H^\alpha$ chemical shifts to the respective random coil values for the peptides huPrP-(110–157) (*white*), huPrP-(140–158) (*black*), and huPrP-(140–166) (*hatched*). *B*, comparison of the $^1H^\alpha$ secondary shifts for the region 140–157. *White bars* correspond to huPrP-(110–157), *black bars* correspond to huPrP-(140–158), and hatched bars correspond to huPrP-(140–166). The *dashed line* at +0.1 ppm indicates the cutoff value for the assignment of extended secondary structure. The *dashed line* at −0.1 ppm indicates the cutoff value for the assignment of helical secondary structure in the regular CSI protocol. *C*, secondary shifts of huPrP-(110–157) in presence of organic co-solvents. Data of huPrP-(110–157) in the presence of 40% acetonitrile are shown in *white* and those in 40% TFE are depicted in *black*.

tion of varying environment, peptides were investigated in the presence of the organic co-solvents trifluorethanol (TFE) and acetonitrile. TFE is known to stabilize the helical conformation of peptides (35), whereas acetonitrile has been shown to enhance fibril formation in peptides (36), presumably by favoring extended conformations. To test whether helix 1 can be further stabilized, huPrP-(140–158) was studied in the presence of 40% TFE at pH 6.5. Judged by the mean residual ellipticity at 222 nm in the CD, the helix content of the peptide has nearly tripled compared with the TFE-free sample at pH 6.5. This finding was confirmed by NMR spectroscopy indicating helical conformation for residues 144–156 with an upfield deviation of the $^1H^\alpha$ resonances, which is on average ~0.5 ppm larger than that for the TFE-free sample (Fig. 1*C*). These observations show that the apparent rise in helix content indicated by CD spectroscopy is attributed to the higher population of helical conformers for residues 145–156 rather than to elongation of helix 1. Because huPrP-(110–157) contains the first β-strand

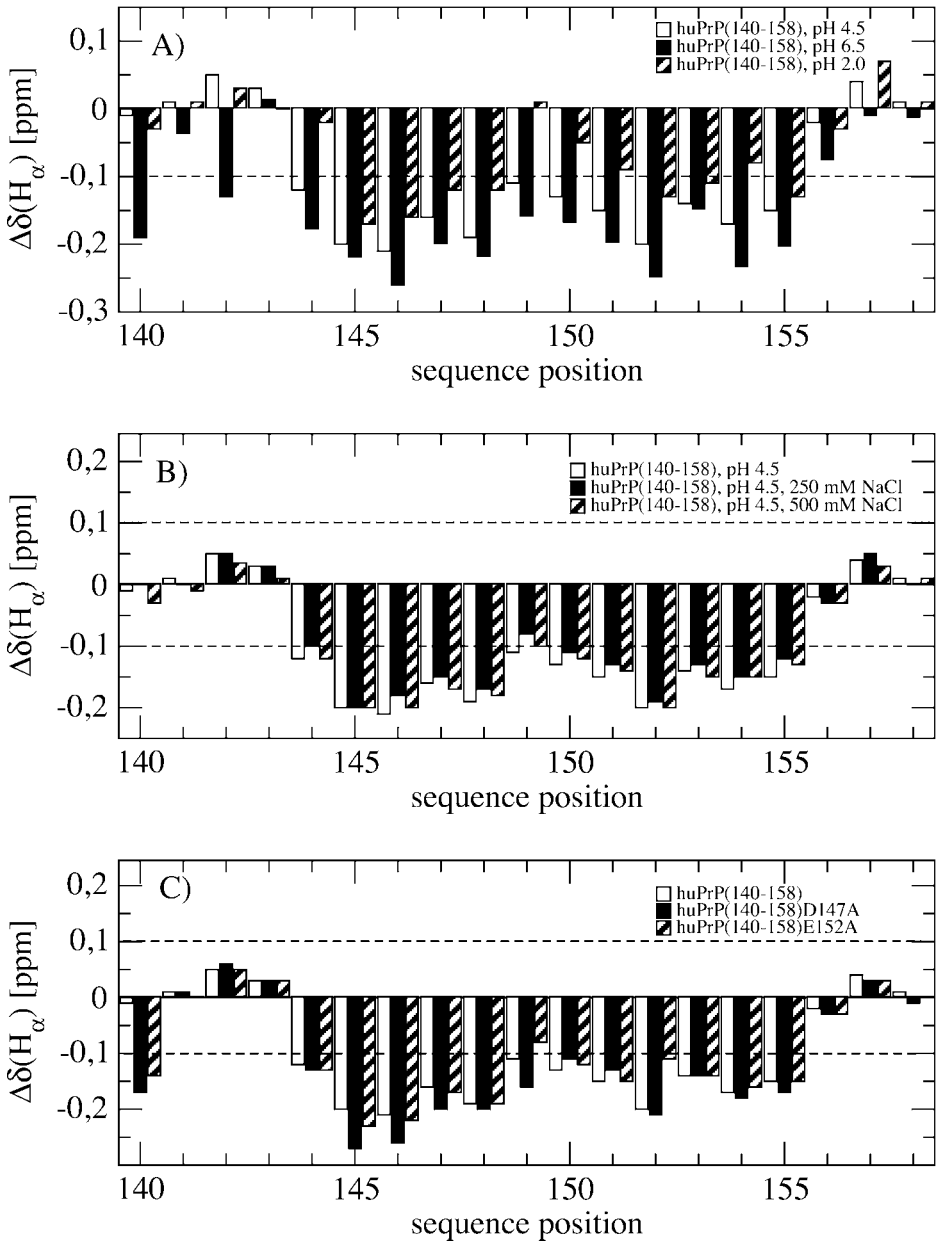

FIG. 2. **Electrostatic influences on $^1H^\alpha$ secondary shifts.** *A*, pH dependency of the $^1H^\alpha$ secondary shifts for huPrP-(140–158). pH 4.5 corresponds to *white bars*, pH 6.5 corresponds to *black bars*, and pH 2.0 corresponds to *hatched bars*. *B*, influence of ionic strength on the $^1H^\alpha$ secondary shifts of huPrP-(140–158). Data at pH 4.5 are shown in the absence of NaCl (*white*) and in the presence of 250 mM NaCl (*black*) and 500 mM NaCl (*hatched*), respectively. *C*, secondary structure shifts of huPrP-(140–158) mutants. $^1H^\alpha$ chemical shifts at pH 4.5 are shown for huPrP-(140–158) wild type (*white*), huPrP(140–158)D147A (*black*), and huPrP(140–158)E152A (*hatched*).

and the potentially amyloidogenic palindrome AGAAAAGA in addition to helix 1, this peptide was investigated in the presence of 40% acetonitrile. However, no evidence for the peptide populating extended conformations (Table I) could be obtained. $^1H^\alpha$ chemical shifts still show helical conformation for residues 145–156 (Fig. 1*C*), but the $^1H^\alpha$ resonances are slightly shifted to lower field compared with the acetonitrile-free sample, indicating destabilization of the helical conformation. Although this finding holds true for the entire sequence, low field shifts were too small to be classified as extended conformations.

Interactions Contributing to the Stability of Helix 1—The sequence of helix 1 exhibits several features that potentially stabilize helical conformations, either by electrostatic (charge-charge or charge-dipole) or by aromatic interactions. Residue Asp-144 acts as a N-cap for the helix stabilizing it by forming a hydrogen bond to an exposed backbone amide located NH_2-terminally of the helix (37). Furthermore, three negative charges (Asp-144, Glu-146, and Asp-147) stabilize helix 1 through favorable electrostatic interactions with the helix dipole. Similarly, the COOH terminus is stabilized by the positive charges of Arg-151, His-155, and Arg-156. In addition, three pairs of oppositely charged amino acids (Asp-147/Arg-151, Asp-144/Arg-148, and Arg-148/Glu-152), each spaced four residues apart in sequence, potentially stabilize helix 1 by the formation of intrahelical salt bridges (38).

Because the stability of helix 1 proved to be insensitive to its immediate sequence neighborhood, further investigations were conducted using the shortest and most soluble peptide, huPrP-(140–158). The contribution of charged residues to helix stability was addressed by changing the pH to 2.0 and 6.5, respectively. CD and NMR spectra at pH 6.5 are similar to those recorded at pH 4.5. Only very small $^1H^\alpha$ shifts to a higher field point toward a marginally more stable helical conformation at pH 6.5 (Fig. 2*A*). In contrast, spectra recorded at pH 2.0 exhibit a marked decrease in helix content (Table I). However, the mean residual ellipticity at 222 nm as well as the $^1H^\alpha$ chemical shifts shows that the peptide retains some residual helicity even under acidic conditions. Chemical shift analysis reveals that no shortening of helix 1 occurs and that no part of the helix is preferentially destabilized. Instead, destabilization to approximately the same extent is observed over the entire helix (Fig. 2*A*). However, over the whole pH range investigated, no

indications for population of extended conformers could be found. None of the NOESY spectra shows long range interactions, again indicating high conformational flexibility.

This pH dependence of helix stability can be attributed to the change in the charge distribution of the peptide. At pH 6.5, all of the acidic and basic residues of the peptide are charged. The negative charges of Asp-144, Glu-146, and Asp-147 as well as the positive charges of Arg-151 and Arg-156 can exert their stabilizing influence on the helix macrodipole. Furthermore, i,i+4 spaced oppositely charged residues potentially form stabilizing salt bridges. Lowering the pH to 4.5 did not lead to significant destabilization, indicating that aspartate and glutamate residues are still carrying negative charges. At pH 2.0, all of the acidic residues are protonated, reducing salt bridges to charge-dipole interactions and charge-dipole to dipole-dipole interactions. This reduction of the strength of attractive electrostatic interactions in combination with repulsion by positively charged residues is suggested to be responsible for the decrease in helix content at pH 2.0.

In particular, the putative salt bridges Asp-147/Arg-151 and Arg-148/Glu-152 are of interest with respect to the stability of helix 1. Therefore, huPrP-(140–158) was investigated at pH 4.5 in the presence of 50, 250, and 500 mM NaCl, respectively. No changes were observed with 50 mM NaCl compared with the salt-free peptide (data not shown). $^1H^{\alpha}$ chemical shifts also indicate helical conformation for residues 145–155 at both higher concentrations of NaCl (Fig. 2*B*). However, the population of the helix is nearly identical to that of the salt-free sample. In particular, the conformation of residues potentially involved in intrahelical salt bridges is not influenced by NaCl concentrations up to 500 mM. This might be because of the mutual cancellation of two opposite effects. Whereas increasing the salt concentration stabilizes helices by screening the helix macrodipole (39), solvent-exposed interactions between charged side chains are weakened at higher ionic strengths. To probe for the role of the putative salt bridges without being influenced by the abovementioned effects, we mutated amino acids contributing to the putative intrahelical salt bridges to huPrP-(140–158)D147A and huPrP-(140–158)E152A. The CD spectrum of huPrP-(140–158)E152A is virtually identical to the spectrum of the wild-type sequence, whereas the spectrum of huPrP-(140–158)D147A even exhibits an increase in helix population as judged from the mean residual ellipticity at 222 nm (Table I). CD results are in good agreement with $^1H^{\alpha}$ chemical shifts analysis. Shifts for residues 145–155 of huPrP-(140–158)D147A (Fig. 2*C*) are nearly identical to the wild-type peptide with the exception of residues Tyr-145, Glu-146, and Ala-147, which are shifted to slightly higher field, indicating a marginally higher population of helical conformers. Similarly, the helix extends from Tyr-145 to His-155 in huPrP-(140–158)E152A. Again, $^1H^{\alpha}$ secondary chemical shifts are comparable with those of the wild-type peptide with the exception of a small downfield shift of approximately 0.05 ppm at the site of the mutation, indicating slight destabilization of the helix at this position (Fig. 2*C*). Helix content and relative secondary shifts for both mutations are consistent with predictions made by AGADIR (Table I) (40, 41, 42).

Disruption of salt bridges by mutation causes destabilization of the helix, which is compensated for by the high helix propensity of the substituent alanine. The effects of the mutations are confined to the immediate vicinity of the site of mutation (Fig. 2). Because the effects at the sites of the mutations are also rather small, indicating practically no change in helix population, experimental helix propensity scales (43) can be employed to estimate the stabilizing energy contributed by the amino acid residue exchanged. Exchange of a charged glutamate with alanine should result in a stabilization of 0.3–0.6 kcal/mol in the absence of additional interresidual interactions. The fact that only a small local destabilization of helix 1 in the E152A peptide was observed therefore implies the existence of a helix-stabilizing interaction in the wild-type peptide being at least equal to the energetic difference in helix propensities between glutamate and alanine. Most probably, this stabilization can be attributed to the putative Arg-148/Glu-152 intrahelical salt bridge. In the case of the D147A mutant, the experimental helix propensity scales predict a stabilization of 0.6–1.10 kcal/mol for the aspartate-alanine exchange. Although a slight stabilization is observed for this mutant, a more pronounced gain in local helicity is expected in the absence of any stabilizing interactions of Asp-147. However, because AGADIR predicts a stabilizing effect for Arg-151, the potential binding partner of Asp-147, a salt bridge Asp-147/Ar-151 is likely to exist. Our results are in line with recently published unfolding data on the Syrian hamster PrP-(23–231) mutants Asp^{144}-(Asn/Ala) and $Asp\text{-}^{147}$(Asn/Ala), respectively, which do not lead to significant destabilization of the full-length prion protein but exhibit an increased conversion efficiency *in vitro* (44). Most probably, both aspartate residues are involved in local interactions affecting helix stability (Asp-144, N-cap, helix macrodipole; Asp-147, i,i+4 salt bridge), which when disrupted do not cause a global effect on the whole protein but which locally destabilize helix 1, rendering it more susceptible for a conformational change, which in turn may cause the observed differences in conversion efficiency.

Further evidence for the stabilizing effect of i,i+4 charge-charge interactions comes from a pattern search of such interactions in three-dimensional structures deposited in the PDB. Systematic analysis of all of the known structures deposited in the PDB resulted in a total of 2799 hits for the pattern [DE]-*X*-*X*-[DE]-[RK]-*X*-*X*-[RK] and its permutations. >70% of the residues adopt helical conformation. Permutation of charged amino acids in the input pattern resulted in similar helix contents of 64–80% showing that permutation of the charged residues has no significant influence on the preferred type of secondary structure. For that reason, the results from the searches with all four patterns were merged for subsequent analysis.

The highest helical propensity is found for those residues forming the central part of the pattern. Helix propensity steadily decreases toward the ends of the pattern and is significantly lower for the flanking residues (Fig. 3). Approximately 10% of the flanking residues form β-strands while this structural element is almost completely absent (<2%) from the central residues of the pattern. An analysis of structures containing the pattern in a β-sheet conformation is of particular interest with respect to interactions of charged residues in this type of secondary structure and thus to the principles of PrP^{Sc} formation. Interestingly, most structures exhibiting β-sheets in this region do not form one continuous β-strand. Instead, two β-strands in the flanking regions of the pattern are formed while the center part adopts a single turn of helix or a turn connecting both strands, which is consistent with the low β-propensity observed for the middle part of the pattern (Fig. 3). Most of these turns are highly solvent-exposed with the charged side chains pointing out to the solvent instead of showing a regular pattern of intramolecular electrostatic interactions.

The analysis was repeated for the full pattern of potential salt bridge-forming residues ([DE]-*X*-*X*-[DE]-[RK]-*X*-*X*-[RK]-[DE]) without permutations, yielding a total of 146 hits. No significant influence of the additional charge could be observed. The proportion of residues in helical conformation still amounts to 77%. To assess the effects of point mutations dis-

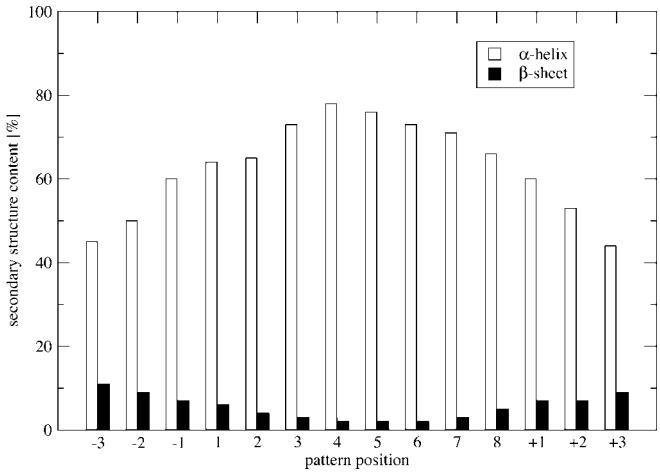

FIG. 3. **Helix and sheet propensities of residues forming the pattern [DE]-*X*-*X*-[DE]-[RK]-*X*-*X*-[RK].** Positions 1–8 indicate the residues 1–8 of the pattern, positions −3 to −1 indicate the three residues preceding the pattern, and positions +1 to +3 indicate the three residues following the pattern. Helix and sheet propensities were calculated from all of the known protein structures containing the pattern as described under "Experimental Procedures."

rupting the salt bridge network, the patterns [DE]-*X*-*X*-A-[RK]-*X*-*X*-[RK]-[DE] modeling the D147A mutation and [DE]-*X*-*X*-[DE]-[RK]-*X*-*X*-[RK]-A modeling the E152A mutation were analyzed using the same procedure. The number of hits decreased to 53 for the D147A pattern and 39 for the E152A pattern. The probability of finding residues of these patterns in helical conformation is nearly unchanged in comparison to the wild-type pattern (83% for D147A and 77% for E152A). Again, the central part of the pattern has the lowest probability to adopt extended conformations, whereas this probability rises toward the termini of the pattern. However, the small number of occurrences of the mutations in the patterns points toward an involvement of these residues in salt bridge-like interactions.

Although electrostatic interactions play an important role in helix 1, they are unlikely to be the sole reason for the high helix content in PrP helix 1. It has been shown that i,i+4 hydrophobic interactions stabilize helices (28, 45, 46). PrP helix 1 contains a pair of i,i+4-spaced tyrosine residues in positions 145 and 149, respectively. In the NMR structure of human PrP, the aromatic side chains are oriented perpendicular toward each other (8). Most probably, an aromatic ring hydrogen of Tyr-149 binds to a carbon of the aromatic ring of Tyr-145 in a weak hydrogen bond-like interaction (47, 48). A stabilizing interaction of Tyr-145 and Tyr-149 could be confirmed by AGADIR. The sequence of the peptide under investigation also contains Phe-141, which potentially could interact with Tyr-145. Despite not being part of the helix in either the NMR structure of the entire protein or the isolated peptide, Phe-141 forms an aromatic interaction similar to Tyr-145/Tyr-149 with Tyr-150. Thus, a cluster of aromatic residues is formed in the peptide, which is solvent-exposed to a large part even in the structure of PrP. In addition to its importance for the stability of helix 1 itself and for the attachment of helix 1 to helices 2 and 3, this cluster of aromatic residues may play an important role for the binding of potential therapeutic drugs such as quinacrine (49).[2]

Our data underline the importance of interleaved placement of i,i+4 electrostatic and aromatic interactions for the formation of stable helices. However, close inspection of the chemical shifts in helix 1 reveals that the helix is more stable at its termini than in its central part. A steric reason might be the proximity of two tyrosine residues in the central part that carry large bulky side chains. Recently, it has been shown that sequences containing residues with bulky side chains in close proximity have a tendency to adopt extended conformations in disordered polypeptides to minimize repulsion because of sterical hindrance (50). The local destabilizing character of Tyr-150 is underlined by AGADIR, which predicts an increase in helix population of 60% for a Y150A mutation.

The Interactions Rendering PrP Helix 1 Stable Are Responsible for Residual Helicity and Turn Formation in Disordered States—Residual helicity is retained even under denaturing conditions because it was also observed in a highly polar region (E52-AEMKA-S58) in acid-unfolded and in urea-denatured apomyoglobin (45, 50). Remarkably, this sequence, which includes helix D of apomyoglobin, has an even higher content of residual helix than helix H of apomyoglobin, which has been shown to have a very high intrinsic helix propensity in peptide studies. Similar to helix 1 of PrP, a pattern of favorable i,i+4 interactions between charged and other polar residues (Lys^{50}-Glu^{54}, Glu^{52}-Lys^{56}, Glu^{54}-Ser^{58}) can be found. In addition, non-polar i,i+4 interactions are present (Thr^{51}-Met^{55}, Ala^{53}-Ala^{57}, Ala^{57}-Leu^{61}). In contrast to PrP helix 1, charges in this sequence of apomyoglobin do not favorably interact with the helix macrodipole and the non-polar interactions do not involve aromatic residues, which in summary is likely to result in the higher helix propensity of PrP helix 1. Interestingly, high residual helix contents can also be observed in the polar sequence stretch M57-SEED-L62 of unfolded apo-plastocyanin (51). In contrast to apo-myoglobin, this sequence codes for a loop in the native protein, indicating that highly polar amino acid sequences exhibit a strong helix-forming tendency *per se*. However, another short peptide from apomyoglobin spanning the CD turn forms a turn conformation in aqueous solution that includes a strong salt bridge (Asp-44/Arg-47). Therefore, polar sequence patterns are not only involved in helix formation, they may also contribute to turn formation. This is in line with our findings from the pattern searches that in cases of non-helical conformers the central part of helix 1 forms a turn in most cases.

Implications for the Conversion Reaction—Our observations consequently lead to the question of how helix 1, although being remarkably stable against environmental and mutational changes, is involved in the conformational conversion of PrP^{C} to PrP^{Sc}. In particular, helix 1 has to undergo complete structural rearrangement from helical conformation to a β-sheet conformation according to recent structural model derived from cryoelectron crystallography of two-dimensional crystals of prion protein (15). In view of its high stability, it is highly unlikely that helix 1 acts as initial starting point for the conversion as proposed previously (16). Because helix 1 is embedded in parts in the structure that already adopt in large part a β-sheet or extended conformation in PrP^{C}, it is likely that this helix is one of the final parts of prion protein that changes its structure in a local unfolding event. Thus, helix 1 may actually delay propagation of a structural change that is initiated somewhere else in the protein. This is in agreement with mutation studies in which helix 1 was deleted (PrP-(121–231)-ΔH1 (52) and PrP106 (53)). In both cases, strongly decreased stability was observed. In particular, PrP106 is largely unstructured and precipitates spontaneously forming β-sheet conformations. Moreover, it could recently be shown that the monoclonal antibody ICSM 18, which recognizes residues 146–159 of murine PrP^{C}, inhibits prion replication and delays development of prion disease (54).

In this context, it is interesting to observe that chemical

[2] A. Frank, J. Ziegler, P. Rösch, and S. Schwarzinger, unpublished observations.

shifts of residues immediately preceding helix 1, in particular His-140 and Gly-142, indicate the presence of some helical structure at pH 6.5 (Fig. 2*A*). This residual helicity is lost upon decreasing the pH to 4.5, thereby increasing conformational flexibility in this part of the protein, which suggests that the protonation state of His-140 might influence the secondary structure in this region. In fact, peptides that contain the bulky residues IIHF immediately preceding Gly-142, but do not include helix 1, form fibrils more readily than for example peptides containing only the alanine-rich part preceding the COOH-terminal domain of PrP.[3] This raises the possibility for a mechanism of PrP^{Sc} formation in which a nucleus for oligomerization is formed by hydrophobic contacts at solvent-exposed parts of the protein, such as I138-IHF or β-strand 1 (Tyr-128-ML). Contact formation and subsequent extension of the β-sheet nucleus lead to a change in the chemical environment of helix 1 causing it to unfold at least partially and change into a conformation presumably consisting of sheet- and turn-elements. The conversion may be further facilitated by changes in the environment such as a decrease of the pH.

Summary—We showed that helix 1 is remarkably stable over a wide range of conditions. No set of solvent conditions applied was sufficient to completely disrupt the helical conformation. As the model of PrP^{Sc} devised by Wille *et al.* (15) proposes the incorporation of helix 1 into the parallel β-helix forming the main part of prion amyloid, the high stability of helix 1 could be part of a barrier needed to prevent the spontaneous conversion of PrP^{C} to PrP^{Sc} (55). Conversion of helix 1 into an extended sheet structure is possibly induced by means of a changed tertiary environment after the prion transformation has been initiated in some other part of the protein. The nature of this initiation site, however, remains unclear. For both regions proposed to be involved in the early stages of transformation, the stretch of apolar residues in the region 110–120 (12, 33) and the short anti-parallel β-sheet of the prion protein, no indication for the existence of stable extended conformers could be found. This might be because of the higher flexibility of the used model peptides compared with the full-length prion protein in which where tertiary interactions stabilize the two β-strands of PrP^{C}. In addition, we show that helix 1 can be further stabilized by TFE despite its high intrinsic stability. The potential for additional stabilization makes helix 1 an interesting target for drug design. For example, short model peptides like huPrP-(140–158) could be used to assess potential helix-stabilizing effects of agents discussed for anti-prion medications.

REFERENCES

1. Prusiner, S. B. (1998) *Proc. Natl. Acad. Sci. U. S. A.* **95,** 13363–13383
2. Wopfner, F., Weidenhofer, G., Schneider, R., von Brunn, A., Gilch, S., Schwarz, T. F., Werner, T., and Schatzl, H. M. (1999) *J. Mol. Biol.* **289,** 1163–1178
3. Suzuki, T., Kurokawa, T., Hashimoto, H., and Sugiyama, M. (2002) *Biochem. Biophys. Res. Commun.* **294,** 912–917
4. Brown, D. R. (2001) *Brain. Res. Bull.* **55,** 165–173
5. Martins, V. R., Linden, R., Prado, M. A., Walz, R., Sakamoto, A. C., Izquierdo, I., and Brentani, R. R. (2002) *FEBS Lett.* **512,** 25–28
6. Pan, K. M., Baldwin, M., Nguyen, J., Gasset, M., Serban, A., Groth, D., Mehlhorn, I., Huang, Z., Fletterick, R. J., Cohen, F. E., and Prusiner, S. B. (1993) *Proc. Natl. Acad. Sci. U. S. A.* **90,** 10962–10966
7. Prusiner, S. B., McKinley, M. P., Bowman, K. A., Bolton, D. C., Bendheim, P. E., Groth, D. F., and Glenner, G. G. (1983) *Cell* **35,** 349–358
8. Zahn, R., Liu, A., Luhrs, T., Riek, R., von Schroetter, C., Lopez Garcia, F., Billeter, M., Calzolai, L., Wider, G., and Wüthrich, K. (2000) *Proc. Natl. Acad. Sci. U. S. A.* **97,** 145–150
9. Riek, R., Hornemann, S., Wider, G., Glockshuber, R., and Wüthrich, K. (1997) *FEBS Lett.* **413,** 282–288
10. Lopez Garcia, F., Zahn, R., Riek, R., and Wüthrich, K. (2000) *Proc. Natl. Acad. Sci. U. S. A.* **97,** 8334–8339
11. Donne, D. G., Viles, J. H., Groth, D., Mehlhorn, I., James, T. L., Cohen, F. E., Prusiner, S. B., Wright, P. E., and Dyson, H. J. (1997) *Proc. Natl. Acad. Sci. U. S. A.* **94,** 13452–13457
12. Jobling, M. F., Stewart, L. R., White, A. R., McLean, C., Friedhuber, A., Maher, F., Beyreuther, K., Masters, C. L., Barrow, C. J., Collins, S. J., and Cappai, R. (1999) *J. Neurochem.* **73,** 1557–1565
13. Jamin, N., Coic, Y. M., Landon, C., Ovtracht, L., Baleux, F., Neumann, J. M., and Sanson, A. (2002) *FEBS Lett.* **529,** 256–260
14. Hornemann, S., Korth, C., Oesch, B., Riek, R., Wider, G., Wüthrich, K., and Glockshuber, R. (1997) *FEBS Lett.* **413,** 277–281
15. Wille, H., Michelitsch, M. D., Guenebaut, V., Supattapone, S., Serban, A., Cohen, F. E., Agard, D. A., and Prusiner, S. B. (2002) *Proc. Natl. Acad. Sci. U. S. A.* **99,** 3563–3568
16. Morrissey, M. P., and Shakhnovich, E. I. (1999) *Proc. Natl. Acad. Sci. U. S. A.* **96,** 11293–11298
17. Fernandez, A. (2002) *Eur. J. Biochem.* **269,** 4165–4168
18. Edelhoch, H. (1967) *Biochemistry* **6,** 1948–1954
19. Sklenar, V., Piotto, M., Leppik, R., and Saudek, V. (1993) *J. Magn. Reson. A* **102,** 241–245
20. Liu, M., Mao, X., Ye, C., Huang, H., Nicholson, J. K., and Lindon, J. C., (1998) *J. Magn. Reson. A* **132,** 125–129
21. Hwang, T. L., and Shaka, A. J. (1995) *J. Magn. Res. Ser. A* **112,** 275
22. Braunschweiler, L., and Ernst, R. R. (1983) *J. Magn. Reson.* **53,** 521–528
23. Bodenhausen, G., Kogler, H., and Ernst, R. R. (1984) *J. Magn. Reson.* **58,** 370–388
24. Van Geet, A. L. (1970) *Anal. Chem.* **42,** 679–680
25. Friedrichs, M. S. (1995) *J. Biomol. NMR* **5,** 147–153
26. Wüthrich, K. (1986) *NMR of Proteins and Nucleic Acids*, John Wiley & Sons, Inc., New York
27. Wishart, D. S., Sykes, B. D., and Richards, F. M. (1992) *Biochemistry* **31,** 1647–1651
28. Schwarzinger, S., Kroon, G. J., Foss, T. R., Chung, J., Wright, P. E., and Dyson, H. J. (2001) *J. Am. Chem. Soc.* **123,** 2970–2978
29. Schwarzinger, S., Kroon, G. J., Foss, T. R., Wright, P. E., and Dyson, H. J. (2000) *J. Biomol. NMR* **18,** 43–48
30. Wishart, D. S., Bigam, C. G., Holm, A., Hodges, R. S., and Sykes, B. D. (1995) *J. Biomol. NMR* **5,** 67–81
31. Chen, Y., Yang, J. T., and Chau, K. H. (1974) *Biochemistry* **13,** 3350–3359
32. Kabsch, W., and Sander, C. (1983) *Biopolymers* **22,** 2577–2637
33. Gasset, M., Baldwin, M. A., Lloyd, D. H., Gabriel, J. M., Holtzman, D. M., Cohen, F. E., Fletterick, R., and Prusiner, S. B. (1992) *Proc. Natl. Acad. Sci. U. S. A.* **89,** 10940–10944
34. Chakrabartty, A., Kortemme, T., Padmanabhan, S., and Baldwin, R. L. (1992) *Biochemistry* **32,** 5560–5565
35. Buck, M. (1998) *Q. Rev. Biophys.* **31,** 297–355
36. Zhang, H., Kaneko, K., Nguyen, J. T., Livshits, T. L., Baldwin, M. A., Cohen, F. E., James, T. L., and Prusiner, S. B. (1995) *J. Mol. Biol.* **250,** 514–526
37. Richardson, J. S., and Richardson, D. C. (1988) *Science* **240,** 1648–1652
38. Marqusee, S., and Baldwin, R. L. (1987) *Proc. Natl. Acad. Sci. U. S. A.* **84,** 8898–8902
39. Scholtz, J. M., York, E. J., Stewart, J. M., and Baldwin, R. L. (1991) *J. Am. Chem. Soc.* **113,** 5102–5104
40. Munoz, V., and Serrano, L. (1994) *Nat. Struct. Biol.* **1,** 399–409
41. Munoz, V., and Serrano, L. (1995) *J. Mol. Biol.* **245,** 275–296
42. Munoz, V., and Serrano, L. (1995) *J. Mol. Biol.* **245,** 297–308
43. Pace, C. N., and Scholtz, J. M. (1998) *Biophys. J.* **75,** 422–427
44. Speare, J. O., Rush, T. S., III, Bloom, M. E., and Caughey, B. (2003) *J. Biol. Chem.* **278,** 12522–12529
45. Yao, J., Chung, J., Eliezer, D., Wright, P. E., and Dyson, H. J. (2001) *Biochemistry* **40,** 3561–3571
46. Butterfield, S. M., Patel, P. R., and Waters, M. L. (2002) *J. Am. Chem. Soc.* **124,** 9751–9755
47. Shoemaker, K. R., Fairman, R., Shultz, D. A., Robertson, A. D., York, E. J., Steward, J. M., and Baldwin, R. L. (1990) *Biopolymers* **29,** 1–11
48. Armstrong, K. M., Fairman, R., and Baldwin, R. L. (1993) *J. Mol. Biol.* **230,** 284–291
49. Korth, C., May, B. C., Cohen, F. E., and Prusiner, S. B. (2001) *Proc. Natl. Acad. Sci. U. S. A.* **98,** 9836–9841
50. Schwarzinger, S., Dyson, H. J., and Wright, P. E. (2002) *Biochemistry* **41,** 12681–12686
51. Bai, Y., Chung, J., Dyson, H. J., and Wright, P. E. (2001) *Protein Sci.* **10,** 1056–1066
52. Eberl, H., and Glockshuber, R. (2002) *Biophys. Chem.* **96,** 293–303
53. Baskakov, I. V., Aagaard, C., Mehlhorn, I., Wille, H., Groth, D., Baldwin, M. A., Prusiner, S. B., and Cohen, F. E. (2000) *Biochemistry* **39,** 2792–2804
54. White, A. R., Enever, P., Tayebi, M., Musheens, R., Linehan, J., Brandner, S., Anstee, D., Collinge, J., and Hawke, S. (2003) *Nature* **422,** 80–83
55. Eigen, M. (1996) *Biophys. Chem.* **63,** A1–A18

[3] J. Ziegler, P. Rösch, and S. Schwarzinger, unpublished results.